

A Discontinuous Galerkin Finite Element Approach for the EEG Forward Problem

Vorwerk, J.¹, Engwer, C.², Ludewig, J.^{1,2}, Wagner, S.¹, Wolters, C.H.¹

¹Institute for Biomagnetism and Biosignalanalysis, Westfälische Wilhelms-Universität Münster, Germany

²Institute for Computation and Applied Mathematics, Westfälische Wilhelms-Universität Münster, Germany

j.vorwerk@uni-muenster.de

Introduction

The accuracy that can be achieved in EEG source analysis strongly depends on an accurate solution of the respective forward problem. Numerical approaches are needed to compute the head surface potential distributions resulting from dipolar current sources when using realistically shaped volume conductor models of the human head (Wolters et al., 2007). Here, we have implemented and evaluated a **Discontinuous Galerkin Finite Element Method** (DG-FEM) to solve the EEG forward problem. In contrast to Continuous Galerkin FEM (CG-FEM, a.k.a conforming or Lagrange FEM), DG-FEM uses basis functions that are only supported on one element each. This leads to discontinuities over element borders (Engwer, 2009; Ludewig, 2013). Continuity and boundary conditions are only enforced weakly through penalty terms on element interfaces and on the boundary.

Motivations for the use of DG-FEM are

- **mass conservation** properties, and thereby
- prevention of **leakage effects** (as they were shown by Sonntag, DGBMT 2013)
- handling of **non-conforming meshes**, enabling unfitted DG (Nüßing, BaCI 2015)
- simple matrix structure enabling easy **parallelization**

Methods

We implemented the Subtraction DG-approach in the **DUNE**¹-framework (for basic formulas see Nüßing, BaCI 2015). We used a variety of 4-layer sphere models **seg_x_res_y** (radii 78, 80, 86, 92 mm, conductivities 0.33, 1.79, 0.01, 0.43 S/m) for validation. Furthermore, we used models with a thinner skull compartment to **enforce leakages** denoted **seg_2_res_2_rx**.

Models **seg_x_res_y** (Fig. 1)

x - segmentation accuracy, x = 1,2,4 mm

y - mesh resolution, y = 1,2,4 mm, y ≤ x

Models **seg_2_res_2_rx** (Fig. 5, left column)

2 mm segmentation accuracy and mesh resolution

x - radius of the outer skull

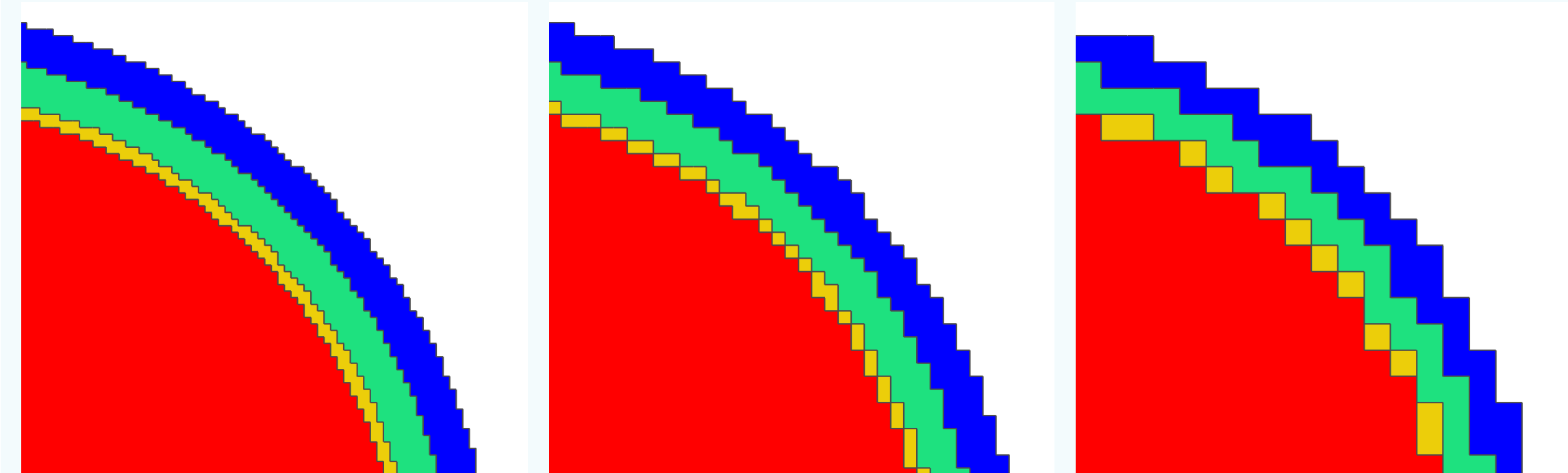
seg_2_res_2_r82 has 10,080 leaks, seg_2_res_2_r83 1,344 leaks

We distributed dipoles with radial orientation up to an **eccentricity of 0.993**, i.e., 0.5 mm below the brain/CSF interface. At each eccentricity 10 dipoles were randomly distributed. We used an analytical solution as reference to compute the error measures

RDM (topography error, 0 ≤ RDM ≤ 2) and **InMAG** (log-magnitude error, 0 = no error)

Figure 1

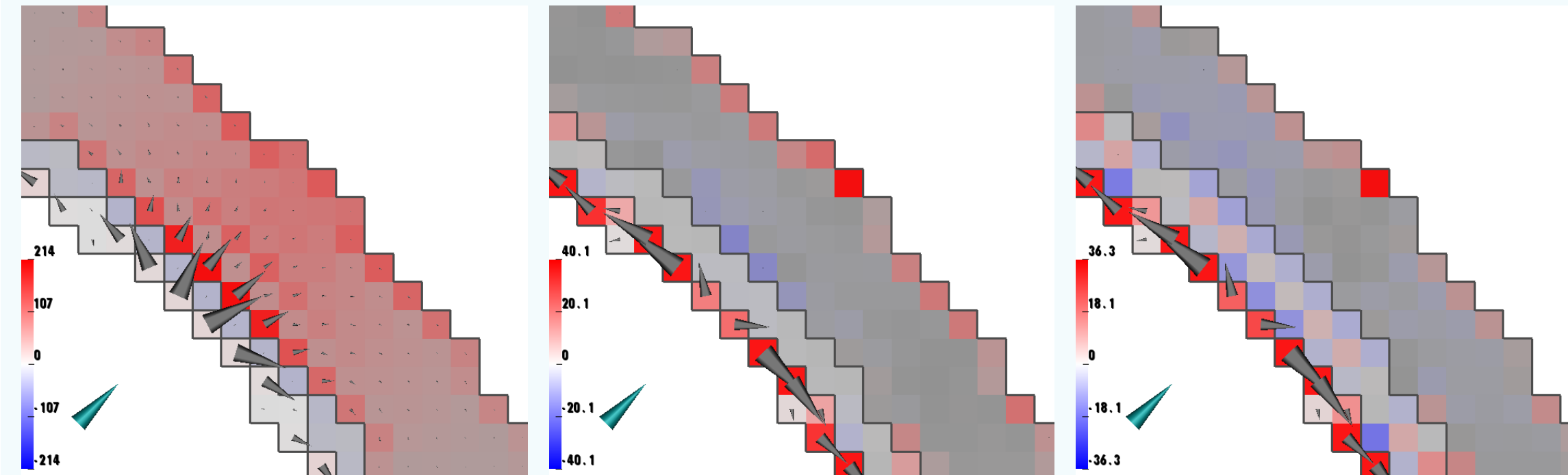
seg_1_res_1 seg_2_res_2 seg_4_res_4



Visualization of used models, cut in x-plane at the origin; coloring is brain - red, CSF - yellow, skull - green, skin - blue.

Figure 6

seg_2_res_2_r82 seg_2_res_2_r83 seg_2_res_2_r84



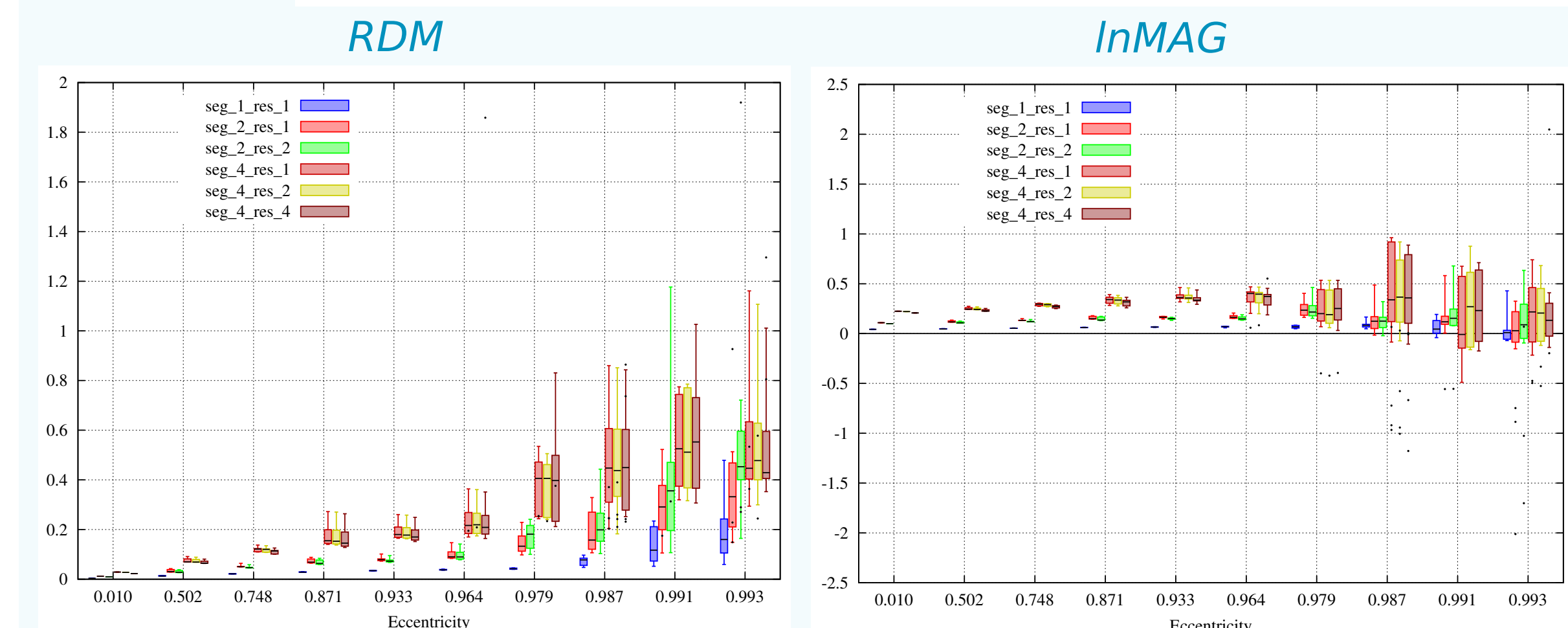
Visualization of current flow differences between CG- and DG-FEM in models. The coloring shows the increase/decrease of the current strength simulated with the CG- compared to the DG-FEM solution in percent; for all models the maximum of the color scale is chosen as the maximal value in the skin and skull compartment. Grey cones show the absolute difference in current flow and have the same, linear scaling for all models. The arrows in skin and skull are not visible due to the relatively small values. Dark gray lines mark compartment boundaries.

Discussion and Conclusion

We presented numerical experiments for a Subtraction DG-approach. The DG-outperformed the CG-FEM for low mesh resolutions and in "leaky" scenarios, while the two approaches had similar accuracies for high mesh resolutions.

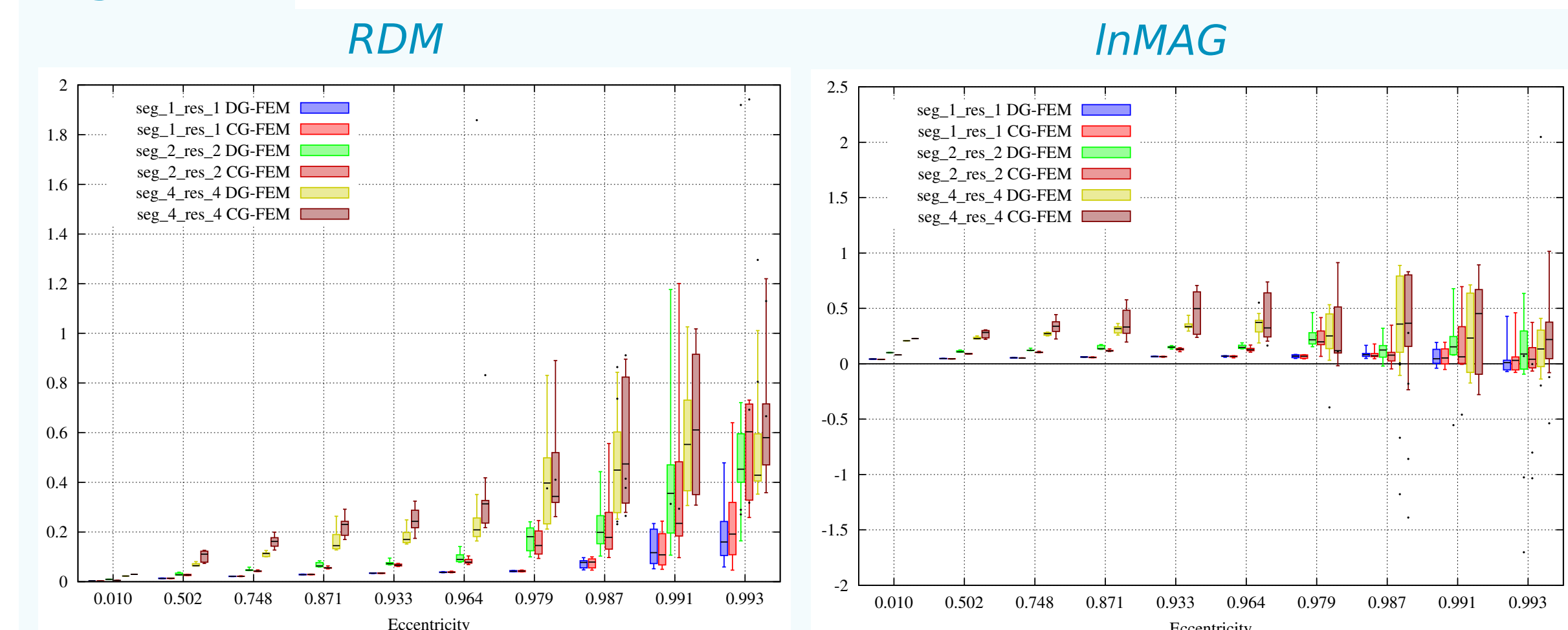
Future work will concentrate on the adaptation of different source models (Venant, Partial Integration) to the DG-framework and the implementation and evaluation of cut-cell approaches that might help to tackle the problem of high errors due to insufficient geometry representation for coarse meshes (Nüßing, BaCI 2015)

Figure 2



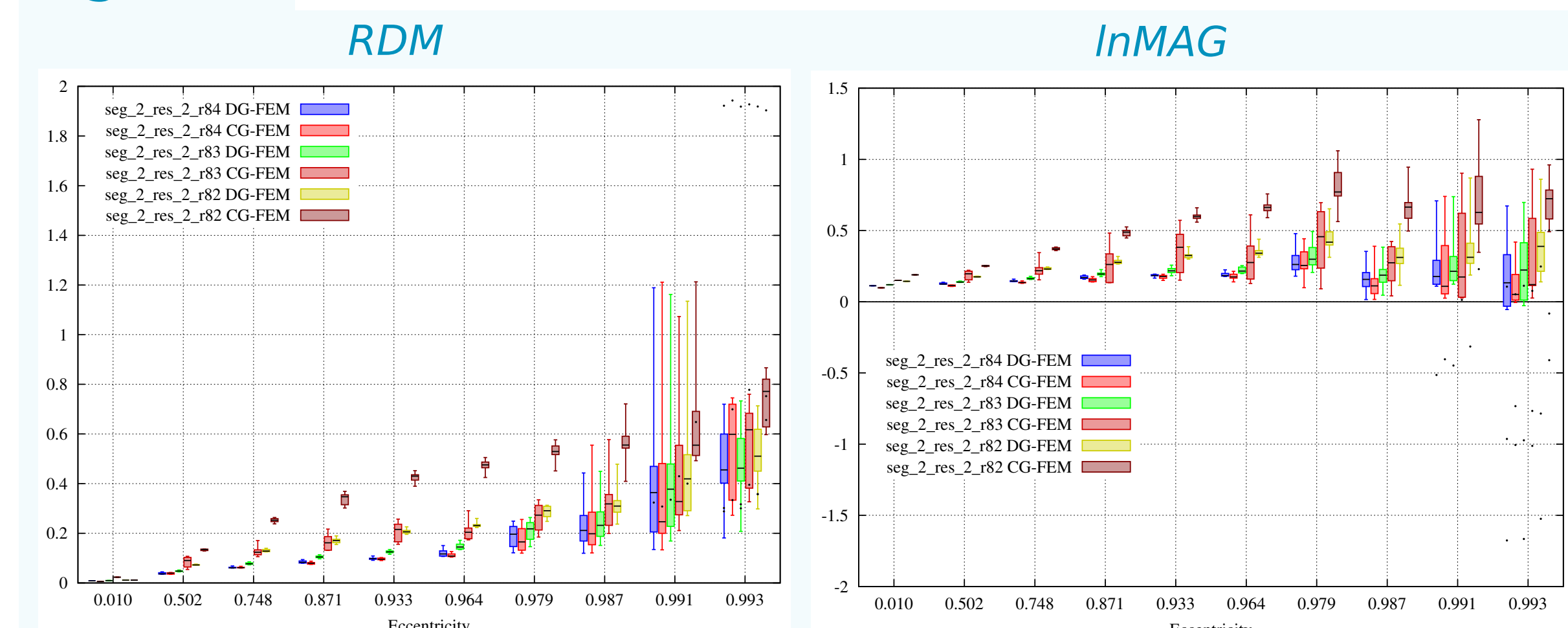
Convergence for DG-FEM with increasing mesh and/or geometrical resolution. Dipole positions that are outside the brain compartment in the discretized models are marked as dots.

Figure 3



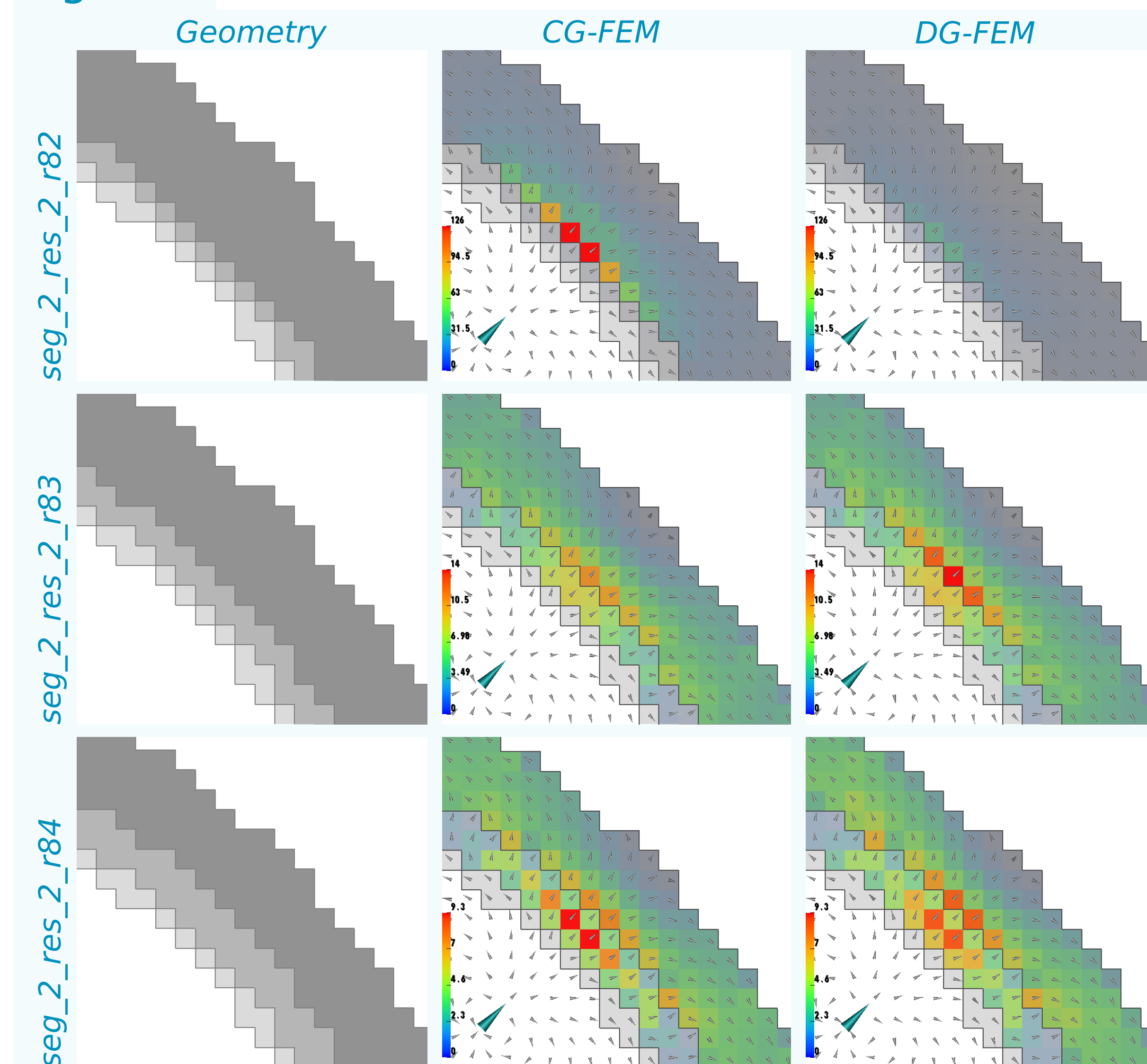
Convergence for CG- and DG-FEM with increasing mesh and geometrical resolution. Dipole positions that are outside the brain compartment in the discretized models are marked as dots.

Figure 4



Errors for models with decreasing skull thickness for CG-FEM and DG-FEM. Dipole positions that are outside the brain compartment in the discretized models are marked as dots.

Figure 5



Visualization of model geometry (left column), current direction and strength for CG-FEM (middle column) and DG-FEM (right column). The left column shows the model geometry, interior to exterior from bottom left to top right, brain, CSF, skull and skin, and air in white. The small and normalized grey cones show the directions of the current flow and, for elements belonging to skull and skin compartments, the coloring indicates the current strength. For each model the color scale is kept constant for both approaches. Dark gray lines mark compartment boundaries.

Wolters et al. (2007) Numerical mathematics of the subtraction approach for the modeling of a current dipole in EEG source reconstruction using finite element head models. *SIAM J. on Scientific Computing*.

Ludewig (2013) Discontinuous Galerkin Methods for the EEG forward problem. *Master Thesis in Mathematics, WWU Münster*.

Engwer (2009) An Unfitted Discontinuous Galerkin Scheme for Micro-scale Simulations and Numerical Upscaling. *PhDthesis, Ruprecht-Karls-Universität Heidelberg*.

Sonntag et al. (2013) Leakage effect in hexagonal fem meshes of the eeg forward problem. *International Conference on Basic and Clinical Multimodal Imaging (BaCI)*.

Nüßing et al. (2015) The Unfitted Discontinuous Galerkin Method in Brain Research. *International Conference on Basic and Clinical Multimodal Imaging (BaCI)*.

¹ <http://www.dune-project.org>, DUNE, a free and open-source modular C++ toolbox for solving partial differential equations using grid-based methods.

Acknowledgement: This research was supported by the Priority Program 1665 of the Deutsche Forschungsgemeinschaft (DFG) (project WO1425/5-1) and by the EU project ChildBrain (Marie Curie Innovative Training Networks, grant agreement no. 641652).